Supplementary Material to the article "Random laser generation under dissipative tunneling in a network quantum material"

1. MAIN EQUATIONS

This section discusses the derivation and justification of the main Eqs.(2) represented in the main part of the article.

Let us first assume that tunneling parameter J is real, which corresponds to Hermitian Hamiltonian (1) in the paper. In this case, to obtain the basic equations, one can use the Heisenberg-Langevin approach (see, for example, [1]), which is quite universal in describing laser-like effects occurring in a two-level system (TLS), cf. [2]. In this case, based on Hamiltonian (1), operator equations are obtained in the form

$$\dot{\hat{f}}_i = -(i\omega_{ph,i} + \kappa_i)\hat{f}_i - ig\hat{\sigma}_i^- + iJ\sum_{j=1}^{N}\tau_{ij}\hat{f}_j + \hat{F}_{ph,i}; \tag{S1a}$$

$$\dot{\hat{\sigma}}_i^- = -(i\omega_0 + \Gamma)\hat{\sigma}_i^- + ig\hat{\sigma}_i^z\hat{f}_i + \hat{F}_{-,i}; \tag{S1b}$$

$$\dot{\hat{\sigma}}_i^z = (\gamma_P - \gamma_D) - (\gamma_P + \gamma_D)\hat{\sigma}_i^z + 2ig(\hat{f}_i^\dagger\hat{\sigma}_i^- - \hat{f}_i\hat{\sigma}_i^+) + \hat{F}_{z,i}, \tag{S1c}$$

where the following notations are introduced: Γ is the rate of decay of TLS polarization, which we assume to be the same for all TLSs; κ_i is the rate of photon loss in the i-th microcavity (MC); γ_P is the pumping rate; γ_D is the population inversion decay rate. Quantum effects occurring in an open dissipative-pumped system are also taken into account in (S1a)-(S1c) by the presence of Langevin force operators $\hat{F}_{ph,i}$, $\hat{F}_{-,i}$ $\hat{F}_{z,i}$.

Under consideration of quantum effects, the corresponding operators of physical quantities are called $\hat{\sigma}_i^\pm \simeq \langle\hat{\sigma}_i^\pm\rangle + \delta\hat{\sigma}_i^\pm$, $\hat{\sigma}_i^z \simeq \langle\hat{\sigma}_i^z\rangle + \delta\hat{\sigma}_i^z$, $\hat{f}_i \simeq \langle\hat{f}_i\rangle + \delta\hat{f}_i$, where operators $\delta\hat{\sigma}_i^\pm$, $\delta\hat{\sigma}_i^z$, $\delta\hat{f}_i$ characterize small quantum fluctuations of physical quantities relative to their average values $\langle\hat{\sigma}_i^\pm\rangle$, $\langle\hat{\sigma}_i^z\rangle$, $\langle\hat{f}_i\rangle$, respectively, cf. [2]. In the semiclassical limit, which is of interest in this work, in (S1a)-(S1c) quantum fluctuations of all physical quantities should be neglected, as well as correlations of Langevin force operators. In this case, we are dealing with the *mean field approximation* for the system of operator Eqs.(S1a)-(S1c), when operators $\hat{\sigma}_i^z$, $\hat{f}_i, \hat{f}_i^\dagger, \hat{\sigma}_i^\pm$ are replaced by their averages. It is worth mention that the averages of the Langevin force operators are equal to zero, i.e. $\langle\hat{F}_{ph,i}\rangle = \langle\hat{F}_{-,i}\rangle = \langle\hat{F}_{z,i}\rangle = 0$. As a result, from (S1a)-(S1c) we obtain

$$\langle\dot{\hat{f}}_i\rangle = -(i\omega_{ph,i} + \kappa_i)\langle\hat{f}_i\rangle - ig\langle\hat{\sigma}_i^-\rangle + iJ\sum_{j=1}^{N}\tau_{ij}\langle\hat{f}_j\rangle; \tag{S2a}$$

$$\langle\dot{\hat{\sigma}}_i^-\rangle = -(i\omega_0 + \Gamma)\langle\hat{\sigma}_i^-\rangle + ig\langle\hat{\sigma}_i^z\rangle\langle\hat{f}_i\rangle; \tag{S2b}$$

$$\langle\dot{\hat{\sigma}}_i^z\rangle = (\gamma_P - \gamma_D) - (\gamma_P + \gamma_D)\langle\hat{\sigma}_i^z\rangle + 2ig(\langle\hat{f}_i^\dagger\rangle\langle\hat{\sigma}_i^-\rangle - \langle\hat{f}_i\rangle\langle\hat{\sigma}_i^+\rangle). \tag{S2c}$$

By introducing the appropriate notation $\mathcal{E}_i = \langle\hat{f}_i\rangle$, $\bar{P}_i = \langle\hat{\sigma}_i^-\rangle$, $\sigma_i^z = \langle\hat{\sigma}_i^z\rangle$ for averages of operator quantities, as well as discarding "fast" oscillations by substituting $\bar{P}_i(t) \to \bar{P}_i e^{-i\omega_0 t}$, $\mathcal{E}_i(t) \to \mathcal{E}_i e^{-i\omega_0 t}$ we then arrive to Eqs.(2) in the main text of the article.

In the work, stationary solutions of Eqs.(2) are considered in the dissipative tunnelling limit. We consider parameter J to be complex, i.e. $J = J_R + iJ_I$, as part of our phenomenological approach. In particular, the substitution of J into Eq.(2a) from the main part of the article allows us to express it in the form

$$\dot{\mathcal{E}}_i = -\kappa_i\mathcal{E}_i - J_I\sum_{j=1}^{N}\tau_{ij}\mathcal{E}_j - i\left(\Delta_i\mathcal{E}_i + g\bar{P}_i - J_R\sum_{j=1}^{N}\tau_{ij}\mathcal{E}_j\right). \tag{S3}$$

It is clear from (S3) that parameter J_R determines the coherent effects of photon tunnelling between MCs in the considered approximation (in (S3) it is included in the Hermitian part in the parentheses). In contrast, J_I defines incoherent phenomena. These can be caused, for example, by inhomogeneities and disorder in the medium that supports photon tunnelling between the microcavities. In particular, the photon loss during tunnelling was considered in the problem of laser generation in the system of nonequilibrium and spatially disordered Bose-Einstein condensate of exciton-polaritons, see [3]. In their work, the authors tried to justify the coherent field equations obtained in the mean field approximation (see for example (8) in [3]), and they also proposed the concept of weak lasing due to the effects of dissipative tunneling of photons between islands of disordered condensate. This approach is suitable when the nonequilibrium system as a whole is close to the threshold of lasing. However, for more complex open (non-Hermitian) systems, to which the model considered in this work belongs, and which may exist in states far from the threshold, a phenomenological approach that considers the balance between the classical effects of dissipation and gain is appropriate; this approach is commonly used in the description and analysis of modern spatially distributed photonic systems with field generation and attenuation effects, see [4, 5]. Thus, analysis of Eqs.(2) in our work follows the phenomenological approach.

2. SPECTRAL PROPERTIES OF THE PHOTON NETWORK STRUCTURE INCLUDING TUNNELLING DISSIPATION EFFECTS

To identify the effect of dissipation in the tunnelling of photons on the spectral properties of the photon network (PN) determined by a random graph in Fig. 1 (see main text of the article), consider the limit where the tunnelling parameter J is significantly larger than the rest of the system parameters and formally we can assume $\Delta_i, \kappa_i, g_i = 0$. In this case, Eq.(4a) of the main text takes the form

$$\omega E_i + J\sum_{j=1}^{N}\tau_{ij}E_j = 0, \quad i = 1, ..., N, \tag{S4}$$

where $\mathbf{T} \equiv \{\tau_{ij}\}$ is the adjacency matrix; ω specifies set of eigenfrequencies of the random laser; E_i describes the amplitude of the stationary EM field in the i-th network node oscillating at frequency ω.

Fig. S1 shows the dependence of the eigenfrequencies of a random laser in the considered limit as a numerical solution of Eqs. (S4). In particular, these dependencies correspond to those for the upper-frequency branch in Fig. 2 of the main text of the article and are plotted with the same values of tunnelling parameters $J^{(1)}$ and $J^{(2)}$. From Fig. S1, it can be seen that for $J^{(1)} = J_R$, in the absence of any dissipation effects, all eigenfrequencies are valid and lie on the line $\mathrm{Im}(\omega) = 0$. With $J_I > 0$ for $J^{(2)} = J_R + iJ_I$, the spectrum is also on a straight line but rotated by a certain angle Θ, relative to the abscissa axis.

Mathematically, Eqs. (S4) represent an eigenvectors-eigenvalues problem of adjacency matrix $\mathbf{T}$, multiplied by complex number $-J$, i.e. $\mathbf{T}' = -J\mathbf{T}$. Due to the properties of the solutions of such a problem one should assume that the eigenvalues are also multiplied by the same number, see e.g. [6]. However, the eigenvectors of both $\mathbf{T}$ and $\mathbf{T}'$ matrices do not change. Thus, substituting $J^{(1,2)}$ in (S4) for this set of eigenvectors $\{E_i\}$, we obtain two sets of eigenfrequencies $\omega^{(1,2)}$ in the form:

$$\omega^{(1)}E_i = -J^{(1)}\sum_{j=1}^{N}\tau_{ij}E_j; \tag{S5a}$$

$$\omega^{(2)}E_i = -J^{(2)}\sum_{j=1}^{N}\tau_{ij}E_j, \quad i = 1, ..., N, \tag{S5b}$$

where $J^{(1)} = J_R$, $J^{(2)} = J_R + iJ_I$. Subtracting (S5a) from (S5b), and also taking into account that $i\Omega = \omega^{(2)} - \omega^{(1)}$ we obtain

$$\Omega = -J_I e^{i(\chi_i - \phi_i)}\frac{|\bar{E}_i|}{|E_i|} \equiv -J_I\eta e^{i(\chi_i - \phi_i)}, \tag{S6}$$

where $E_i = |E_i|e^{i\phi_i}$; ϕ_i is the phase in the i-th MC.

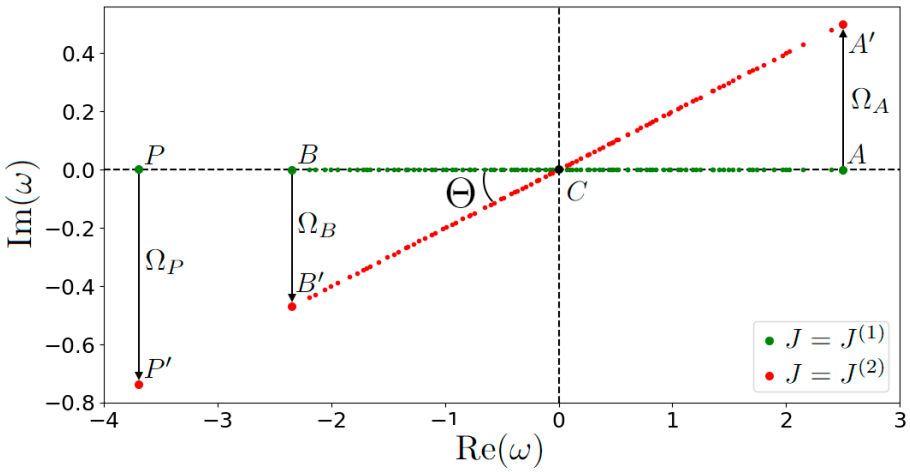

Fig. S1. The eigenfrequencies of a random laser based on the PN graph considered in Fig. 1 at $J^{(1)} = 0.5$ and $J^{(2)} = 0.5 + 0.1i$. Other parameters are $\kappa_i = \Gamma = \Delta_i = g_i = 0$, $N = 100$. The bold green dots represent Perron frequency P, second frequency (after Perron) A, second minimum frequency B, and zero frequency C, respectively. Similar frequencies for the red bold dots are indicated by capital letters with primes. Ω_P, Ω_A, and Ω_B are the offsets along the ordinate axis for the imaginary part of the characteristic frequencies, taking into account the effects of dissipation in the presence of tunnelling of photons between MCs.

In (S6), we defined the local average field acting on the i-th node from its neighbours as

$$\bar{E}_i = \sum_{j=1}^{N} \tau_{ij} E_j = |\bar{E}_i| e^{i\chi_i}, \tag{S7}$$

where χ_i is the phase of the local average field of neighbours in the i-th MC.

It is important to note that the sum in (S7) contains only k_i terms, which is significantly less than N due to the sparsity of adjacency matrix $\mathbf{T}$. In other words, for a given i-th node, the non-zero elements of the sum in (S7) are only the j-th nodes associated with the i-th one, since only for them $\tau_{ij} = 1$. Effective parameter $\eta = |\bar{E}_i|/|E_i|$ in (S6) defines the amplitude of the local average field of the i-th MC neighbours related to the amplitude of its field. Physically, η specifies influence of neighbouring MCs to the tunnely coupled i-th MC. The numerical calculation shows that for each of the random laser modes, the η parameter is the same for all nodes.

Fig. S2 shows the dependencies of the eigenvalues of fields E_i $(i = 1, ..., N)$ corresponding to the eigenfrequencies indicated in Fig. S1 by the dots P', A', B' (for dots P, A, B, and C field amplitudes E_i are the same). Notice, in the analyzed limit, all amplitudes E_i are real, i.e., the radiation of a random laser is linearly polarized.

Fig. S3 exhibits the graph of the PN of a random laser, coloured depending on the value of the field amplitudes E_i in the nodes $i = 1, ..., N$ for the same dependencies as in Fig. S2. This allows us to highlight the "brightest" nodes that will contribute the most to the radiation of a random laser when the corresponding mode is amplified. It is important to note that the brightest node's degree for the Perron frequency is maximal and equal to $k_i = 13$, see Fig. S3(a). For the frequencies shown in Fig. S1, dots A' and B' have also large connectivity values $k_i = 12$, see Fig. S3(b, c) However, for dot C' the brightest MC is only connected with two MCs in the PN, i.e. $k_i = 2$, see Fig. S3(d).

As seen from Fig. S2(a), field amplitudes E_i at the network nodes $i = 1, ..., N$ for Perron frequency ω_P are positive, which is a consequence of the Frobenius-Perron theorem [7]. In this case, the influence of neighbours tunnelly coupled with some i-th MC for a given mode is maximal, $\eta_P = 7.38$, and $\Phi_i \equiv \chi_i - \phi_i = 0$ for all i, that is the fields E_i and $\bar{E}_i$ are in phase, and $\Omega_P = -J_I \eta_P$. On the other hand, for the Perron frequency we can use the annealed network approximation by setting $\tau_{ij} = k_i k_j / N\langle k \rangle$. Physically, this approximation means that the

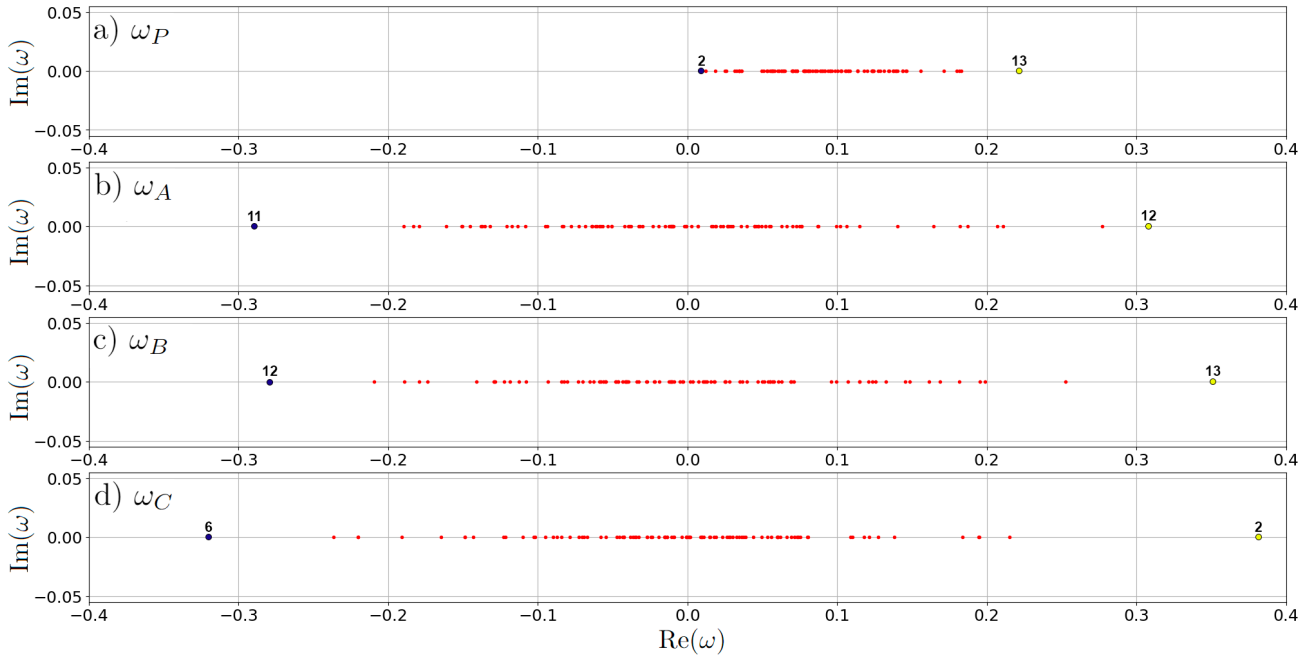

Fig. S2. Amplitudes of stationary fields E_i in the random laser nodes for (a) the Perron frequency (dot P in Fig. S1), (b) the second highest frequency (dot A in Fig. S1), (c) the second minimum frequency (dot B in Fig. S1), and (d) zero frequency (dot C in Fig. S1), respectively. The parameters of the system are the same as for Fig. S1; $J^{(2)} = 0.5 + 0.1i$. Blue and yellow dots mark the minimum and maximum field amplitudes for each case (in Fig. S3 these amplitudes correspond to the nodes of the same colours). The numbers above the dots indicate degrees k_i of these nodes.

effective local average field at an arbitrary i-th node is determined by the global average (over the network) field $\bar{E}$, so that $\bar{E}_i = k_i \bar{E}$, where

$$\overline{E} = \frac{1}{N\langle k\rangle} \sum_{j=1}^{N} k_j E_j. \tag{S8}$$

Then (S6) takes a form

$$\Omega = -J_I \eta_P = -J_I \zeta, \tag{S9}$$

which gives us $\eta_P = \zeta$.

Thus, the sign of Ω, which determines the amplification ($\Omega > 0$) or diminishing ($\Omega < 0$) of the field energy at frequency ω, directly depends on the relative phases of the fields at the nodes, $\Phi_i = \chi_i - \phi_i$. Namely, from Fig. S1 it follows that $\Omega < 0$ for all eigenfrequencies such that $\mathrm{Re}(\omega) < 0$. Physically, this means that for characteristic eigenfrequencies lying to the left of value $\mathrm{Re}(\omega) = 0$, the average field and the fields at the nodes are in phase, i.e. $\Phi_i \simeq 0$ and $E_i \simeq \zeta|\bar{E}_i|$.

This physical situation is illustrated in Fig. S3. As example, we take the i-th MC in the node located on the right side of the analyzed PN graph. This i-th MC is tunnelly coupled with two other MCs, as seen from Fig. S3; the numbers in the figures indicate the field values in all three MCs (graph nodes). From Fig. S3(a) it is clear that for the Perron frequency the field values in all these MC (nodes) are positive, i.e. are in phase, see also Fig. S2.

Similar behaviour is demonstrated by the second minimum frequency - dots, B and B', in Fig. S1. As seen from Fig. S2(c), there are approximately equal number of positive and negative E_i, but they are distributed differently across the network nodes. Namely, fields E_i are distributed so that the intrinsic fields of the nodes are in phase with the local average fields of their neighbours, $\Phi_i = \chi_i - \phi_i = 0$, as for Perron frequency ω_P, see also Fig. S3(c). However, since not all the neighbouring fields are in phase in this case, the influence of neighbours for a given mode is smaller, $E_i \simeq \eta_B|\bar{E}_i|$, where $\eta_B = 4.68$. Using expressions (11) of the main text of the

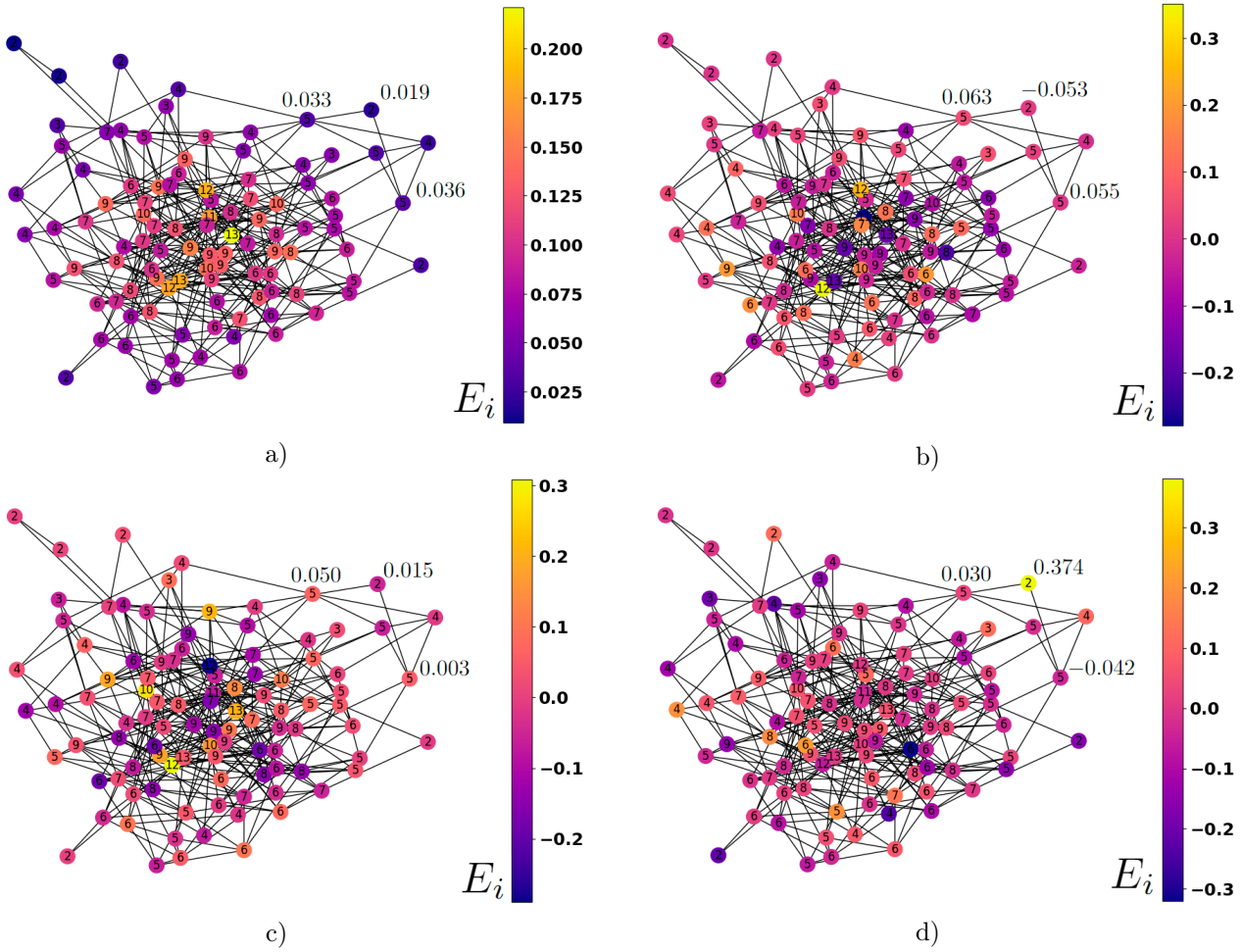

Fig. S3. Graph of the photonic network structure of a random laser, coloured depending on the amplitude of the node eigenfield E_i for (a) the Perron frequency (dot P in Fig. S1), (b) the second highest frequency (dot A in Fig. S1), (c) the second minimum frequency (dot B in Fig. S1), and (d) zero frequency (dot C in Fig. S1). The numbers in the circles indicate degrees k_i of the corresponding nodes. The numbers next to the three connected nodes indicate the value of the field at the corresponding nodes. The system parameters are the same as in Fig. S1, $J^{(2)} = 0.5 + 0.1i$.

article for the typical values of the second minimum frequency in this case, one can obtain $\mathrm{Re}(\omega_B) \simeq -\eta_B J_R$, $\mathrm{Im}(\omega_B) \simeq -\eta_B J_I = \Omega_B$, which allow estimating the angle Θ of the red line in Fig. S1 in the form

$$\tan(\Theta) = \frac{\mathrm{Im}(\omega_B)}{\mathrm{Re}(\omega_B)} = \frac{\Omega_B}{\mathrm{Re}(\omega_B)} = \frac{J_I}{J_R}. \tag{S10}$$

On the contrary, from Fig. S1 it follows that $\Omega_A > 0$ for $\mathrm{Re}(\omega) > 0$. In this case $\Phi_i = \chi_i - \phi_i = \pi$, i.e. local average fields and eigenfields of the nodes are out of phase, $E_i \simeq e^{i\pi}\eta_A|\bar{E}_i|$, where $\eta_A = 4.99$. In particular, it is seen from Fig. S1 for frequency ω_A, whose imaginary part shifts up along the ordinate axis into the lasing region, see (S6) and Fig. S1. From Fig. S3(b) using the example of the i-th MC with field value $E_i \simeq -0.053$, it is clearly seen that the fields from the two neighbouring MCs are out of phase with the i-th one.

Dot C in Fig. S1 remains "fixed" for the value of eignefrequency $\mathrm{Re}(\omega) = 0$, i.e. $\Omega_C = 0$. Since it has the effective local mean field $|\bar{E}_i| \ll |E_i|$, then $\eta_C = 0.036$. In this case, phase difference Φ no longer plays a special role, because the influence of neighbouring MCs is negligible, and the i-th MC can be considered as isolated. In particular, notice the bright yellow node in the upper right part of the graph in Fig. S3(d): this node has the most

intense field E_i precisely because its two adjacent nodes have weak, close in amplitude and opposite in phase fields $E_j \simeq 0.03$ and $E_{j+1} \simeq -0.042$, respectively.

---

1. M. Lax, *Fluctuations and coherence phenomena in classical and quantum physics*, Gordon and Breach, New York (1968).
2. T. Golubeva, Yu. Golubev, D. Ivanov. Phys. Rev. A. **75**, 023815 (2007).
3. I. L. Aleiner, B. L. Altshuler, and Y. G. Rubo, Phys. Rev. B **85**, 121301(R) (2012).
4. C. Wang, Z. Fu, W. Mao, J. Qie, A.D. Stone, and L, Yang, Adv. Opt. Photon. **15**, 442 (2023).
5. S.K. Vadlamani, T.P. Xiao, and E. Yablonovitch, PNAS, **117** (43) 26639 (2020).
6. Gilbert Strang, *Linear algebra and its applications*, Academic Press Inc., New York (1976).
7. C. Sarkar and S. Jalan, Chaos, **28**, 102101 (2018).